

Utilizing Multi-modal Synchrotron Methods for Nuclear Forensic Applications

Simerjeet K. Gill¹, Mehmet Topsakal¹, Ericmoore Jossou¹, David A. Brown¹, Spencer Scott² and Matthew Wellons²

¹Brookhaven National Laboratory, ² Savannah River National Laboratory

Abstract

Constraining the origin and intended use of nuclear materials by rapid, high-sensitivity and high-throughput chemical and structural analysis remains a challenge. High intensity and brightness of third-generation synchrotron sources, such as National Synchrotron Light Source II (NSLS-II), coupled with state-of-the-art sample manipulation and detection tools, present an exceptional opportunity to advance international nuclear forensics capabilities. Synchrotron methods are non-destructive and potentially serve as a unique diagnostic tool by providing not only unique characterization information but also potentially critical downstream analytical operations guidance for subsequent destructive analysis methods. We are developing synchrotron-based methods with several key advantages, including: 1) non-destructive analysis with minimal sample preparation; 2) rapid data collection enabling high sample throughput; 3) focused and high intensity beams resulting in superb spatial resolution and sensitivity; and 4) multi-modality which enables monitoring chemical composition, bulk and local structural changes on the same region of interest in a single measurement. We are developing sample holders that will enable high throughput measurements on different sample types such as capillaries, planchets and swipes and will enable multi-modal measurements so that both bulk structure and sample compositions can be studied via X-ray Diffraction (XRD) and X-Ray fluorescence (XRF) respectively. Our work will provide a comprehensive understanding of actinide-containing particulate systems and enable screening of hundreds of samples per day, which is a significant increase in sample throughput as compared to laboratory-based methods. Our technique will be complementary to existing methods as subsequent isotopic analysis is possible due to the non-destructive nature of analysis.

Introduction

Nuclear forensic science aims to study and evaluate interdicted nuclear or radioactive materials that are discovered outside of regulatory control to constrain the source, history and intended use of the materials¹⁻⁴. The term *nuclear forensics* has been defined as: *the examination of nuclear or other radioactive material, or of evidence that is contaminated with radionuclides, in the context of legal proceedings under international or national law related to nuclear security. The analysis of nuclear or other radioactive material seeks to identify what the materials are, how, when, or where the materials were made, and what their intended uses were*⁵.

Nuclear forensics currently employs analytical methods, such as mass spectrometry (MS), transmission electron microscopy (TEM), scanning electron microscopy (SEM), and Raman spectroscopy (RS), amongst others, to characterize interdicted material at variable spatial scales and degree of analytical precision. Currently, nuclear forensics largely relies on the use of MS techniques which include TIMS⁵, SIMS⁶, and various forms of ICP-MS for identification, isolation, and characterization of radioactive particles⁷. One of the major nuclear forensic applications for MS is the determination of isotopic ratios within a sample, which constrains its provenance, age, and processing history. Mass spectrometric methods offer high precision for isotopic composition and are very valuable for nuclear forensic analysis. However, sample preparation for MS often requires extremely precise separation of analytes^{8,9}. The separations of nuclear samples are particularly challenging due to the complicated mixture of elements that coexist within the material; these are typically a mixture of actinides, decay and fission products, and impurities from mining or milling, and multistep chromatographic separations are often required for quantitative analysis. Consequently, analyte purification can be a lengthy process of manipulations that exploit differences in

solubility, oxidation state, and ligand binding profiles of the many elements present in the sample¹⁰. When working with small quantities of analyte, isotopic carriers are often used to minimize loss of material, but these carriers can render MS measurements more difficult to analyze. These methods are very accurate for isotopic analysis but require either extensive sample preparation (TIMS and ICP-MS) or are limited by lengthy sample analysis times (SIMS). TEM requires laborious sample preparation compared to SEM. These constraints result in longer turnaround periods for data analysts, which slows sample evaluation and response time to decision-making end users.

Although MS is well suited for nuclear forensics, the turnaround time and the destructive nature of the technique is a limiting factor. This is especially true in cases where large sample size can benefit from analysis automation or high-throughput capability. Synchrotron-based analysis is non-destructive and very fast, and hence offer a capability complementary to existing MS techniques, where high precision structural and chemical analysis can be performed by synchrotron while preserving the sample for subsequent detailed isotopic analysis by MS techniques. In addition, the high sensitivity of synchrotron radiation is promising for detecting trace levels of impurities between samples from different sources. For instance, the advanced National Synchrotron Light Source II (NSLS-II) at BNL designed to deliver world-leading intensity and brightness enables the structural and chemical characterization of anthropogenic actinide bearing particles with micron to nanoscale resolution and exquisite sensitivity by providing world-leading capabilities for X-ray diffraction, X-ray fluorescence and X-ray absorption spectroscopy measurements¹¹.

Synchrotron-based XRD was successfully utilized to study the development of various uranium oxide phases as a function of processing conditions, such as relative humidity, temperature, and time, which are parameters that can be used to track origin of uranium oxide^{12,13}. It was reported that while aging time, temperature, and relative humidity all have a quantifiable effect on UO₃ crystallographic and morphological changes, it is relative humidity that had the most significant impact¹³, and was thus most important parameter to track the origin of uranium oxide, which is an important nuclear material for forensics applications. Rapid pre-screening of materials using synchrotron methods could save end-users a significant amount of money in costly and time-consuming laboratory analyses as well as provide complementary analysis to existing destructive analysis techniques such as MS. Synchrotron methods are non-destructive, and samples can be used for isotopic analysis after pre-screening using synchrotron studies. Fast sample turnaround would provide an order-of-magnitude decrease in analysis timeframe; typical sample analyses for uranium may require months to a year with current laboratory queues.

Trace nuclear particulates are extremely challenging analytical specimens due to a combination of potentially multiple chemical species, nuclear material aggregates, inclusion of both natural and anthropogenic non-nuclear debris, and all within micron-sized volumes. Sample evaluation operations routinely work through these challenges by analyzing larger particle populations to establish a preponderance of analytical information. Although an effective brute force solution, it necessitates increased time/budget scope and delays information delivery to end users. The characterization of trace actinide-bearing particulates is an essential component of nuclear forensics and nuclear safeguards analysis. To ensure the veracity of such analysis, high-quality reference materials; namely, particulates with uniform properties, such as size, elemental and isotopic composition, and material phase, are necessary for instrument calibration, method development or benchmarking, and quality control operations. To meet the need for high-quality actinide reference materials, a capability to manufacture microparticulate actinide-bearing particles with tailored size, elemental compositions, isotopic ratios, and material phases has been developed at SRNL and elsewhere. The leading microparticle synthesis methods include hydrothermal chemical synthesis methods^{14,15} and aerosol-based spray drying methods¹⁶. These methods have yielded particulates with a high degree of size and isotopic homogeneity, and, more recently, demonstrated a

capacity for the generation of multi-element particles with known elemental ratios, such as U-Nd¹⁷, U-Ce¹⁸, and U-Th¹⁹. The developed particle generation methods can produce reference particle-laden test specimens across a range of sample types and particle loadings, spanning nanogram to milligram quantities adhered to substrates, cotton swipes, or as powders.

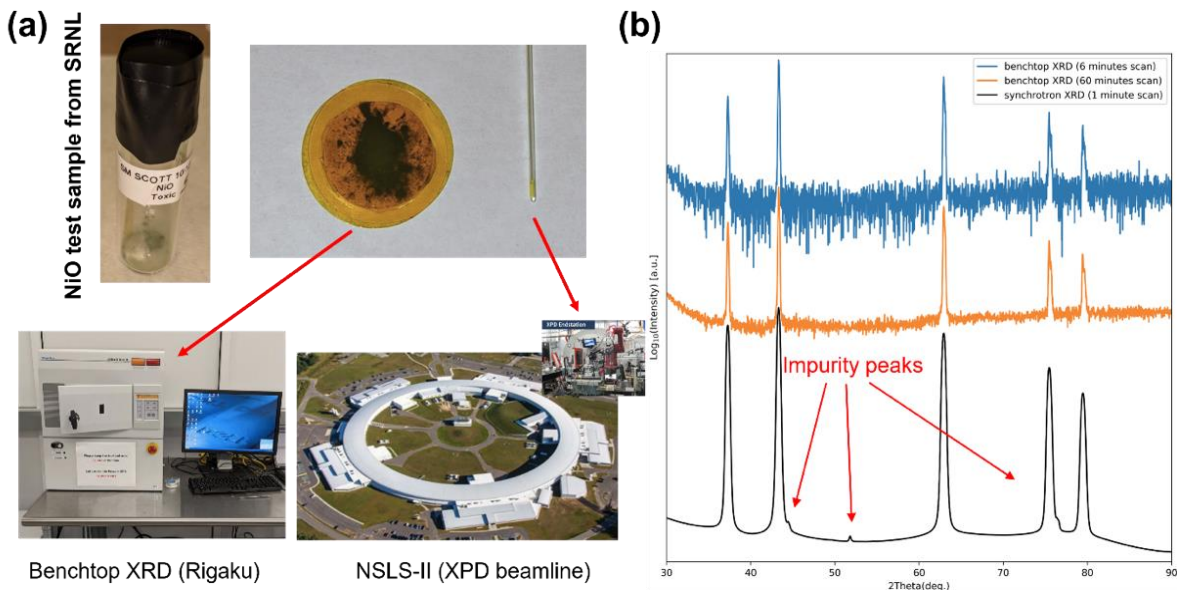


Figure 1: Comparison of benchtop XRD (Rigaku) with synchrotron-based XRD collected at XPD beamline from NSLS-II. (a) NiO sample from commercial vendor is received from SRNL and packed for benchtop and synchrotron measurements in Kapton tape and quartz capillary respectively. (b) Shorter (6 minutes) and longer (60 minutes) benchtop XRD compared with 1 minute synchrotron XRD. Impurity peaks are highlighted with red arrows.

In our current work, we are developing capabilities for high throughput multi-modal studies of actinide containing particulate systems at X-Ray Powder Diffraction (XPD) beamline at National Synchrotron Light Source II (NSLS-II). For this development, we have synthesized high quality surrogate (Cerium oxide based) and actinide (Uranium based) particulate systems at Savannah River National Lab (SRNL) to test and commission the synchrotron-based techniques. The generated particles display a high degree of uniformity with particle sizes near 1 μm as measured by in-situ aerodynamic methods, indicating their suitability of cerium oxide particles as non-radiological surrogates as well as actinide-bearing particles as test materials. Further, we have developed sample holders for capillary, planchet and swipe samples to enable multi-modal high throughput synchrotron studies. Multi-modal data on test materials such as nickel oxide, molybdenum oxide and cerium oxide as well as uranium-based feedstock samples is presented.

Results

Multi-modal synchrotron measurements of surrogate systems.

XRD measurements on various reference powder samples such as NiO, H₂WO₄, MoO₃, WO₂, H₂MoO₄ from commercial vendors and prepared in-house were measured performed at X-Ray Powder Diffraction (XPD) beamline at National Synchrotron Light Source II (NSLS-II) at Brookhaven National Lab (BNL). To demonstrate the sensitivity of the synchrotron based XRD (s-XRD) over typical benchtop XRD setup, we collected XRD data on the commercial NiO powder using a benchtop XRD setup (Rigaku). Figure 1-a shows the NiO sample prepared in-house in lab and packed in Kapton tape for benchtop and synchrotron XRD measurements. Figure 1b clearly demonstrates the advantages of s-XRD against benchtop XRD. Although the 60 minutes benchtop XRD run is significantly improved compared to 6-minutes scan, the 60 minutes benchtop XRD have a significant signal to noise ratio (SNR) compared to the s-XRD. Also,

the s-XRD data was collected in only one minute. Such SNR would make it difficult to detect peaks from impurities with low concentration in particulate samples as demonstrated in Figure 1b. These proof-of-concept measurements demonstrate the high sensitivity of s-XRD due to its better resolution of diffraction peaks than conventional bench top laboratory XRD. The high flux, tunable well-defined wavelength, and better collimation of synchrotron radiation improves the identification of impurities with low concentration. It should also be noted that the number of samples needed for s-XRD is much smaller than the benchtop XRD setup. In addition, the high speed of data collection of s-XRD (1 min) vs benchtop XRD (1 hr) demonstrates that s-XRD is the only path forward to high throughput studies of particulate samples.

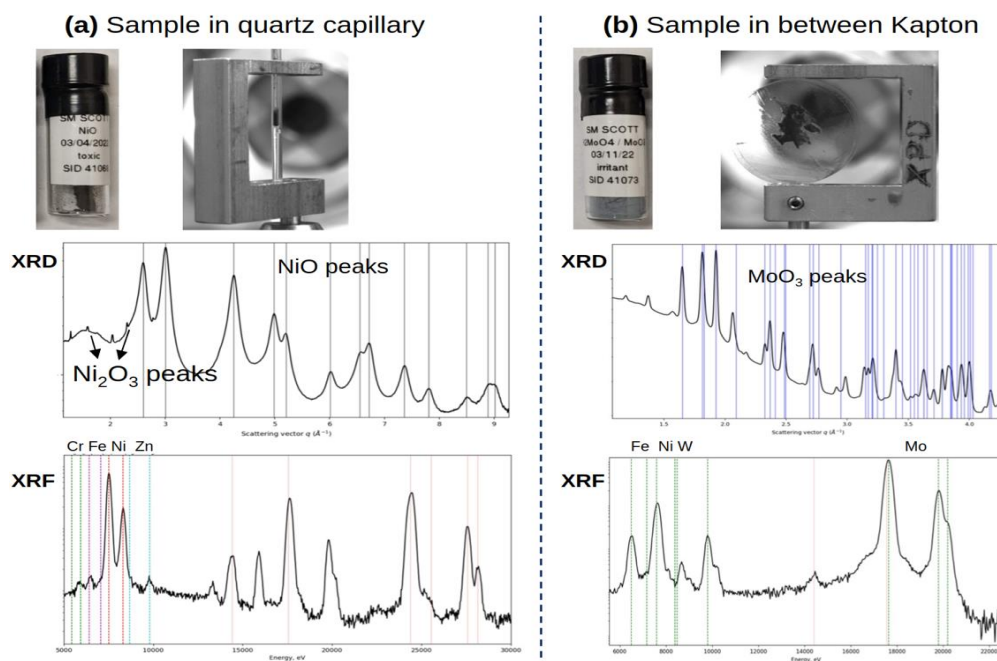


Figure 2: Multi-modal synchrotron XRD & XRF data collected at at XPD beamline at NSLS II on (a) Nickel oxide and (b) Molybdenum oxide test samples received from SRNL.

Multi-modal XRD and XRF data was collected on surrogate nickel oxide and molybdenum oxide powders prepared in lab. We were able to elucidate both the oxide phases and major and minor impurities in the Nickel oxide and Molybdenum Oxide samples. Figure 2a shows NiO sample as prepared in-house and packed in a quartz capillary at BNL. In the XRD profile, NiO (major) and Ni₂O₃ (minor) phases are clearly observable. In addition, XRF analysis confirmed the presence of Cr, Fe, and Zn as major impurities. We did also observe additional minority phases. The molybdenum was placed between two layers of Kapton as shown in Figure 2b. Major MoO₃ peaks are clearly present in XRD profile with Fe, Ni, W impurities in XRF profile.

Capability development for high throughput synchrotron measurements of particulate systems.

We are developing sample holders for synchrotron studies of particulate samples at BNL. An industrial-grade stereolithography (SLA) 3D printer and associated supplies from Formlabs were procured and a new 3D printing area (shown in Figure 3a) was established. The workflow of synthesis of sample holder is shown in Figure 3b. Initially, the sample holder with desired dimensions is designed in a CAD software, which is then fed into 3D printer for manufacturing the holder. Once the holder is printer it is washed with alcohol to clean the holder surface and cured under UV to strengthen the holder.

(a) 3D printing area established in the lab



Figure 3: (a) 3D printing area established in the lab showing the 3D printer, washing as well as curing station for the printed parts. (b) 3D printing workflow for the sample holder printing. (c) an example 3D printed sample holder (on the right) with existing stainless-steel holder (on the left).

(b) Sample holder design and printing workflow (c)



Figure 3c shows an example 3D printed sample holder for samples packed in capillaries. The new design had significant improvement from old stainless-steel holders (shown on the left) as it contains a compartment to secure the sample while transporting and measurement. In addition, hundreds of such holders can be easily printed unlike stainless steel holders, a critical step for enabling high throughput measurements.

Milligram-scale quantities of cerium oxide test particulates for use as non-radiological surrogates in the development of high-throughput synchrotron methods and the qualification of the associated sample holder were synthesized. The cerium oxide particles were generated using the SRNL-developed Thermally Evaporated Spray for Engineered Uniform particles (THESEUS) platform, shown in Figure 4, which utilizes commercially available aerosol instrumentation coupled with SRNL-developed tools for particle collection and containment.

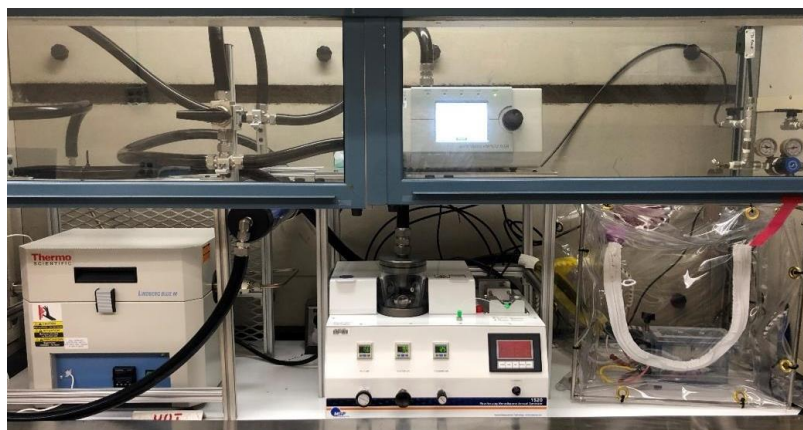


Figure 4: Image of the non-radiological THESEUS platform used in the generation of CeO_2 test particulates.

Cerium oxide particles were generated by heating a dilute cerium nitrate feedstock, with a target CeO_2 particle size of $1 \mu\text{m}$, to 1000°C to ensure conversion to the desired CeO_2 phase. In-situ aerodynamic measurements obtained by Aerodynamic Particle Sizer (APS) indicate a shift in aerodynamic size, above

300 °C, resulting from the change in density associated with the thermal decomposition of cerium nitrate to cerium oxide (Figure 5-A). System stability and particle uniformity during operation was assessed using the APS at startup, refill, shutdown, and at 2-hour intervals during operation. APS results indicate good stability, with a monomodal particle size distribution ($\sigma_G < 1.15$) retained throughout the sustained operations (Figure 5-B).

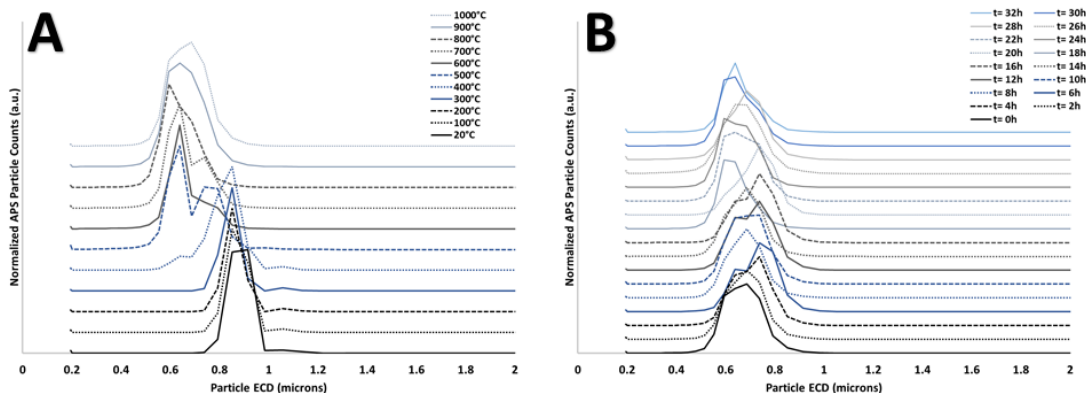


Figure 5: Density-corrected ($\rho = 7.22\text{g/cm}^3$) aerodynamic particle sizing results of CeO_2 particles generated at: (A) varying temperatures, and (B) across multi-day operations.

The generated particles were collected on an electropolished stainless steel plate using an SRNL-developed electrostatic precipitator, and physically harvested (Figure 6-A). A total particle mass of 19.4 mg was collected across 3 multi-day operations. The harvested particles were packaged in glass vials, without any liquid collection media to preserve the particulate qualities (Figure 6-B).

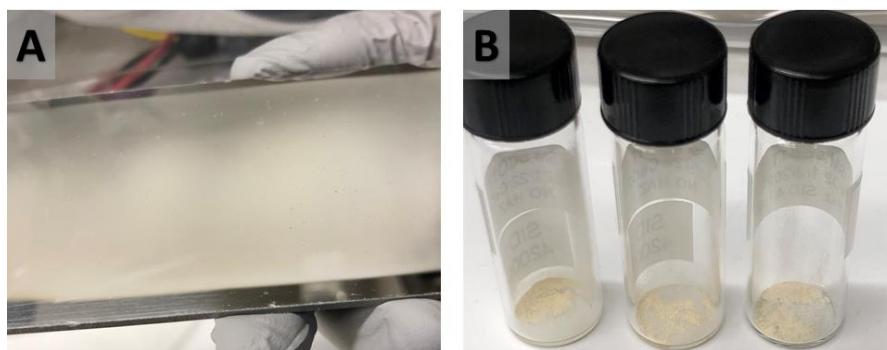


Figure 6: Image of CeO_2 particles: (A) as-collected on a stainless-steel plate, (B) as-harvested in glass vials.

3D printed holders for mounting powder as well as swipe samples for synchrotron studies were designed and developed (Figure 7). The sample holder design and sample mounting were discussed with NSLS II safety team to gain approval for measuring uranium containing samples. Various steps of sample preparation are shown in figure 7. Lab based particulate samples were lifted off from the planchet using a Kapton tape which was applied to blank Kapton tape on the sample holder. After making a sandwich of particulate samples between two Kapton tapes, the sample was further covered with 2 layers of Kapton to meet the requirement of double containment for actinide containing samples for measurements at NSLS II. Once the samples were secured in double containment, they were labeled with unique identification number for easy tracking.

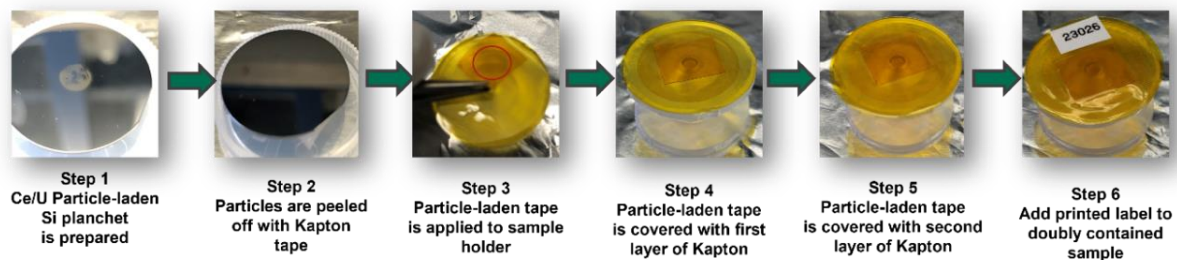


Figure 7: Schematic showing the steps of preparing doubly contained radioactive samples for synchrotron data collection. Samples were mounted to 3D printed holders.

Both cerium-based surrogate and uranium-based actinide samples were prepared in-house, packaged, and shipped to BNL for synchrotron measurements, as shown in Figure 8. The doubly contained samples were secured in magnetic holder and mounted on sample stage at XPD beamline at NSLS II for XRD measurements.

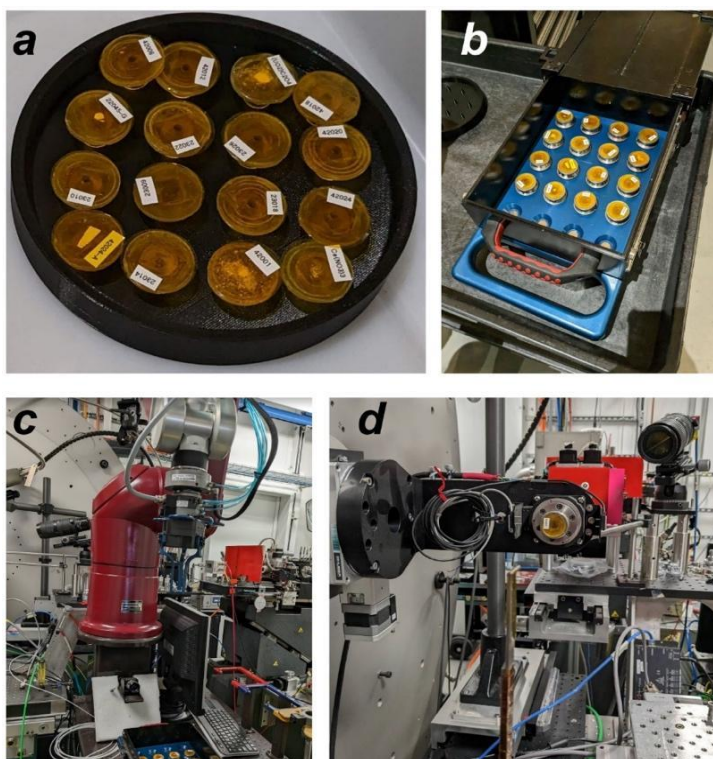


Figure 8: Photographs of the XRD experiment at XPD beamline of NSLS-2. (a) lab synthesized cerium based surrogates and uranium-based actinide samples as received from SRNL. They are placed inside a 3D printed chamber during transport. (b) Samples are placed onto magnetic holders inside a magazine box. Samples are ready to be picked up by the robot arm. (c) Robot arm at the beamline. (d) One of the samples is mounted to the stage and ready for XRD measurement.

Synchrotron based XRD studies for cerium and uranium samples.

Synchrotron based XRD data was collected on doubly contained surrogate and depleted uranium samples. In Figure 9 – left side, lab-synthesized cerium oxide was compared with high-purity (99.99%) cerium oxide from a commercial vendor (Alfa Aesar). Within the detection limits of the technique, it was observed that CeO_2 powder - as synthesized in lab - is clean and does not include impurities or contributions from the feedstock material (cerium nitrate – $\text{Ce}(\text{NO}_3)_3$). It was also observed that the peak widths of lab-synthesized CeO_2 powder are broader compared to commercially available CeO_2 powder with a known particle size of 14 microns. This indicates lower crystallinity and smaller grains in the lab-synthesized CeO_2 . In Figure 10 – right side, XRD profiles of feedstock uranyl oxalate ($\text{UO}_2\text{C}_2\text{O}_4$) and lab-synthesized

triuranium octoxide (U_3O_8) are presented. Although the lab-synthesized U_3O_8 doesn't include phases from feedstock material (uranyl oxalate), there are several peaks in the XRD profile that doesn't belong to hexagonal U_3O_8 . It is important to note that α - U_3O_8 was previously shown to exist at room temperature as a pseudo-hexagonal orthorhombic structure with the space group of $C2mm^{20}$, transforming to a fully stable hexagonal U_3O_8 structure at 483 K with a space group of $P62m$.²¹ These observations underscore the role of the processing routes on the physiochemical properties of the test samples.

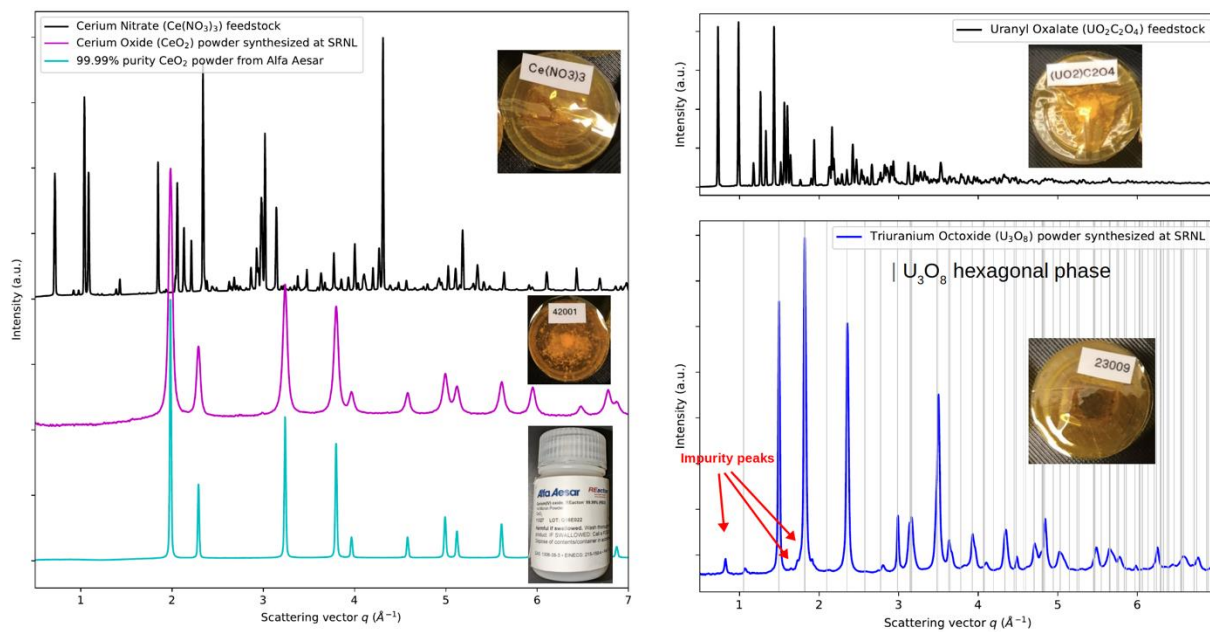


Figure 9 (left) XRD profiles of starting feedstock (cerium nitrate) used for synthesizing CeO_2 , lab-synthesized CeO_2 and CeO_2 from a commercial vendor (Alfa Aesar). (right) XRD profiles of starting feedstock (uranyl oxalate) used for synthesizing U_3O_8 , and lab-synthesized U_3O_8 . Impurity peaks that don't belong to hexagonal U_3O_8 are highlighted by arrows.

Conclusions

This study aims to demonstrate synchrotron studies of particulate samples for nuclear forensics. After initial studies of benchmarking synchrotron XRD and XRF techniques for surrogate nickel oxide and molybdenum oxide particles, we collected data on actinide containing uranium standards using sample preparation protocols for radioactive samples. 3D printed sample holders with doubly contained samples were used to measure XRD data successfully for high-concentration powder samples. This project will specifically confront the technical difficulties of studying actinide-containing particulate samples by advancing high-throughput, multi-modal analysis for combined structural and chemical characterization across length scales, including the development of advanced sample holders for the uranium and plutonium containing samples to be studied at synchrotron facilities. Multi-modal high-throughput capability of analyzing powders is important for allowing for rapid analysis of suspicious materials, environmental samples, or trace contamination on surfaces since powder samples most closely represent field samples (e.g., soil, small particles, debris, etc.). The rapid high-throughput analysis of samples, including nuclear materials, also reduces costs in sample collection, transportation, sample preparation, and analysis time. A deeper comprehension of particulate structure and chemical composition (a function of impurity content and processing conditions, such as uranium particulate synthesis route, calcination temperature, and collection conditions) will strengthen the toolkit for rapid characterization of particulate samples with trace impurities.

Acknowledgements

This manuscript resulted from a collaboration between Brookhaven National Laboratory and Savannah River National Laboratory. Employees of Brookhaven Science Associates, LLC work under Contract No. DE-SC0012704 with the U.S. Department of Energy, and employees of Battelle Savannah River Alliance, LLC work under Contract No. 89303321CEM000080 and/or a predecessor contract with the U.S. Department of Energy. This work was conducted as a part of the National Nuclear Security Administration Defense Nuclear Nonproliferation Research and Development (NNSA DNN R&D) project “Expanding the Nuclear Forensic Toolkit: High-Throughput Synchrotron-Based Studies of Actinide-Containing Reference Particulates”.

References

- (1) Mayer, K.; Wallenius, M.; Ray, I. Nuclear Forensics - A Methodology Providing Clues on the Origin of Illicitly Trafficked Nuclear Materials. *Analyst*. Royal Society of Chemistry 2005, pp 433–441. <https://doi.org/10.1039/b412922a>.
- (2) Mayer, K.; Wallenius, M.; Ray, I. Nuclear Forensics - A Methodology Providing Clues on the Origin of Illicitly Trafficked Nuclear Materials. *Analyst*. Royal Society of Chemistry 2005, pp 433–441. <https://doi.org/10.1039/b412922a>.
- (3) Mayer, K.; Wallenius, M.; Fanghänel, T. Nuclear Forensic Science-From Cradle to Maturity. *Journal of Alloys and Compounds* **2007**, 444–445 (SPEC. ISS.), 50–56. <https://doi.org/10.1016/j.jallcom.2007.01.164>.
- (4) Mayer, K.; Wallenius, M.; Varga, Z. Nuclear Forensic Science: Correlating Measurable Material Parameters to the History of Nuclear Material. *Chemical Reviews*. February 13, 2013, pp 884–900. <https://doi.org/10.1021/cr300273f>.
- (5) Kristo, M. J. Nuclear Forensics Chapter Outline. **2020**. <https://doi.org/10.1016/B978-0-12-814395-7.00013-1>.
- (6) Bürger, S.; Riciputi, L. R.; Turgeon, S.; Bostick, D.; McBay, E.; Lavelle, M. A High Efficiency Cavity Ion Source Using TIMS for Nuclear Forensic Analysis. *Journal of Alloys and Compounds* **2007**, 444–445 (SPEC. ISS.), 660–662. <https://doi.org/10.1016/j.jallcom.2006.11.019>.
- (7) Esaka, F.; Magara, M.; Lee, C. G.; Sakurai, S.; Usuda, S.; Shinohara, N. Comparison of ICP-MS and SIMS Techniques for Determining Uranium Isotope Ratios in Individual Particles. *Talanta* **2009**, 78 (1), 290–294. <https://doi.org/10.1016/j.talanta.2008.11.011>.
- (8) Becker, J. S.; Zoriy, M.; Halicz, L.; Teplyakov, N.; Müller, C.; Segal, I.; Pickhardt, C.; Platzner, I. T. Environmental Monitoring of Plutonium at Ultratrace Level in Natural Water (Sea of Galilee - Israel) by ICP-SFMS and MC-ICP-MS. In *Journal of Analytical Atomic Spectrometry*; 2004; Vol. 19, pp 1257–1261. <https://doi.org/10.1039/b406424k>.
- (9) Lloyd, N. S.; Parrish, R. R.; Horstwood, M. S. A.; Chenery, S. R. N. Precise and Accurate Isotopic Analysis of Microscopic Uranium-Oxide Grains Using LA-MC-ICP-MS. *Journal of Analytical Atomic Spectrometry* **2009**, 24 (6), 752–758. <https://doi.org/10.1039/b819373h>.
- (10) Salbu, B.; Kashparov, V.; Lind, O. C.; Garcia-Tenorio, R.; Johansen, M. P.; Child, D. P.; Roos, P.; Sancho, C. Challenges Associated with the Behaviour of Radioactive Particles in the Environment. *Journal of Environmental Radioactivity* **2018**, 186, 101–115. <https://doi.org/10.1016/j.jenvrad.2017.09.001>.

- (11) Crean, D. E.; Corkhill, C. L.; Nicholls, T.; Tappero, R.; Collins, J. M.; Hyatt, N. C. Expanding the Nuclear Forensic Toolkit: Chemical Profiling of Uranium Ore Concentrate Particles by Synchrotron X-Ray Microanalysis. *RSC Advances* **2015**, *5* (107), 87908–87918. <https://doi.org/10.1039/c5ra14963k>.
- (12) Tracy, C. L.; Chen, C. H.; Park, S.; Davisson, M. L.; Ewing, R. C. Measurement of UO₂ Surface Oxidation Using Grazing-Incidence x-Ray Diffraction: Implications for Nuclear Forensics. *Journal of Nuclear Materials* **2018**, *502*, 68–75. <https://doi.org/10.1016/j.jnucmat.2018.01.052>.
- (13) Hanson, A. B.; Schwerdt, I. J.; Nizinski, C. A.; Lee, R. N.; Mecham, N. J.; Abbott, E. C.; Heffernan, S.; Olsen, A.; Klosterman, M. R.; Martinson, S.; Brenkmann, A.; McDonald, L. W. Impact of Controlled Storage Conditions on the Hydrolysis and Surface Morphology of Amorphous-UO₃. *ACS Omega* **2021**, *6* (12), 8605–8615. <https://doi.org/10.1021/acsomega.1c00435>.
- (14) Barrett, C. A.; Pope, T. R.; Arey, B. W.; Zimmer, M. M.; Padilla-Cintron, C.; Anheier, N. C.; Warner, M. W.; Baldwin, A. A. T.; Bronikowski, M. G.; DeVore II, M.; Kuhne, W.; Wellons, M. S. In *Production of Particle Reference and Quality Control Materials*, 41st ESARADA Conference, December, 2019.
- (15) Spencer M. Scott, Abigail Waldron, Seth Lawson, Michael G. Bronikowski, Laken A. Inabinet, Benjamin E. Naes, Ross J. Smith, Kimberly N. Wurth, Travis J. Tenner, Matthew Wellons. SRNL Report Doc #SRNL-TR-2021-00663, "Production of Mixed Element Actinide Reference Particulates for Nuclear Safeguards Test Materials by an Aerosol Synthesis Method", October 30, 2021.
- (16) Scott, S. M.; Baldwin, A. T.; Bronikowski, M. G.; II, M. A. D.; Inabinet, L. A.; Kuhne, W. W.; Naes, B. E.; Smith, R. J.; Eliel, V.-A.; Tenner, T. J.; Wurth, K. N.; Wellons, M. S., Scale-up And Production Of Uranium-bearing QC Reference Particulates By An Aerosol Synthesis Method. *Proceedings of the Joint INMM & ESARDA 2021 Meeting* 2021.
- (17) Kegler, P.; Pointurier, F.; Rothe, J.; Dardenne, K.; Vitova, T.; Beck, A.; Hammerich, S.; Potts, S.; Faure, A. L.; Klinkenberg, M.; Kreft, F.; Niemeyer, I.; Bosbach, D.; Neumeier, S. Chemical and Structural Investigations on Uranium Oxide-Based Microparticles as Reference Materials for Analytical Measurements. *MRS Advances* **2021**, *6* (4–5), 125–130. <https://doi.org/10.1557/s43580-021-00024-1>.
- (18) Williamson, T. L.; DeVore, M. A.; Tenner, T. J.; Smith, R.; Inabinet, L.; Mershon, J.; Hiller, J.; Wellons, M. S. Towards the Synthesis of Mixed Actinide Particulate Reference Materials: Microscopy and Spectroscopic Characterization of U/Ce-Containing Specimens. *Microscopy and Microanalysis* **2019**, *25* (S2), 1548–1549. <https://doi.org/10.1017/s143192761900847x>.
- (19) SRNL-TR-2021-00663. Production of Mixed Element Actinide Reference Particulates for Nuclear Safeguards Test Materials by an Aerosol Synthesis Method.
- (20) Loopstra, B. O. Crystal-Structure of alpha-U₃O₈. *J. Inorg. Nucl. Chem.* 1977, *39*, 1713–1714. [https://doi.org/10.1016/0022-1902\(77\)80137-1](https://doi.org/10.1016/0022-1902(77)80137-1)
- (21) Wen, X.-D.; Martin, R. L.; Scuseria, G. E.; Rudin, S. P.; Batista, E. R.; Burrell, A. K. Screened Hybrid and DFT+U Studies of the Structural, Electronic, and Optical Properties of U₃O₈. *J. Phys. Condens. Matter* 2012, *25*, 025501. <http://dx.doi.org/10.1088/0953-8984/25/2/025501>